Journal of Hydrology 364 (2009) 107–114

Contents lists available at ScienceDirect

Journal of Hydrology

journal homepage: www.elsevier.com/locate/jhydrol

# Flow in the neighborhood of a confined aquifer observation well

Bwalya Malama *, Warren Barrash

*Center for Geophysical Investigation of the Shallow Subsurface and Department of Geosciences, Boise State University, 1910 University Drive, Boise, ID 83725, USA*

ARTICLE INFO

*Article history:*
Received 24 March 2008
Received in revised form 27 August 2008
Accepted 20 October 2008

*Keywords:*
Observation well
Well hydraulics
Wellbore storage
Confined aquifer
Hydraulic conductivity
Specific storage

SUMMARY

An analytical solution for flow in the vicinity of an observation well is developed. The observation is emplaced in a homogeneous aquifer of infinite radial extent that is pumped at a constant rate, and satisfies the Theis solution. We attempt to account for the effect of an observation well on the drawdown response in a neighborhood of finite radial extent centered around the well. The model of Black and Kipp [Black, J.H., Kipp Jr., K.L., 1977. Observation well response time and its effect upon aquifer tests. Journal of Hydrology 34, 297–306] only makes a correction to the drawdown response at the well location and does not modify the flow pattern in the neighborhood of the well. This may be sufficient for isolated observation wells but, for well-fields or sites with relatively closely spaced wells, the flow patterns in the neighborhoods of the wells may significantly impact drawdown response. The model we develop is applied to field data and is shown to yield an aquifer hydraulic diffusivity that is comparable to that estimated with the model of Black and Kipp [Black, J.H., Kipp Jr., K.L., 1977. Observation well response time and its effect upon aquifer tests. Journal of Hydrology 34, 297–306]. In addition to providing estimates of formation conductivity and specific storage, the solution yield estimates of the hydraulic conductivity and specific storage of the zone of influence and has the ability to predict the effect of the observation well on drawdown response in a finite region of influence in the vicinity of the well.

© 2008 Elsevier B.V. All rights reserved.

## Introduction

It has long been noted that a measuring instrument (observation well or piezometer) emplaced in an aquifer can lead to significant lag, at early-time, of observed drawdown from that predicted by the classical models of Theis (1935) for confined aquifers, and Neuman (1972) for unconfined aquifers. Such a lag, if it is not accounted for in the forward model used in parameter estimation, would lead to significant overestimation of aquifer specific storage (Mucha and Paulikova, 1986). One of the first workers to consider the effect of an observation well or piezometer on measured drawdown was Hvorslev (1951), who introduced the parameter $t_B = C_w/(FK)$ known as the basic time lag of the measuring instrument, where $C_w$ is the instrument storage coefficient, $F$ is the shape factor and $K$ is formation hydraulic conductivity. Papadopulos and Cooper (1967) developed a solution that accounted for the effect of pumping wellbore storage in confined aquifers. Black and Kipp (1977) extended the theory of Hvorslev (1951) to observation wells placed in a confined aquifer that satisfies the solution of Theis (1935). They introduced the dimensionless parameter $\beta = 4\alpha t_B/r^2$ known as the response factor of the measuring instrument, where $\alpha$ is formation hydraulic diffusivity and $r$ is the radial distance from the pumping well. They developed a type-curve method for estimating aquifer parameters.

Boulton and Streltsova (1976) considered the effect of wellbore storage for the problem of flow in unconfined aquifers. However, their solution has the limitation that it does correctly model unconfined aquifer flow since a constant head boundary condition was imposed at the watertable. Narasimhan and Zhu (1993) developed a numerical model to account for wellbore storage effects in unconfined aquifers considering both the approaches of Boulton (1954) and Neuman (1972) for accounting for delayed gravity response. Moench (1997) developed an analytical model that accounts for both pumping well and observation well storage effects in unconfined aquifers, using a boundary condition at the watertable that can be shown to lead to the model of Boulton (1954) for vertically averaged flow, and to the linearized kinematic condition used by Neuman (1972) under the assumption of instantaneous watertable drainage. To account for observation well storage effects, Moench (1997) adopted the approach of Black and Kipp (1977).

It should be noted that in the model of Hvorslev (1951) and Black and Kipp (1977), a small jump discontinuity exists across the interface between wellbore and formation fluid as can be seen in Fig. 1a, which is a schematic of the conceptual model adopted by Black and Kipp (1977) for drawdown in the wellbore and in the formation. In the figure, the dashed curve represents the Theis (1935) solution, and the solid curve is the solution of Black and Kipp (1977). Note that in the formation, the two solutions coincide. To resolve the difficulty presented by the jump discontinuity in head at the wellbore–formation boundary it is necessary to introduce

* Corresponding author. Tel.: +1 208 426 2959; fax: +1 208 426 3888.
*E-mail address:* bmalama@cgiss.boisestate.edu (B. Malama).

0022-1694/$ - see front matter © 2008 Elsevier B.V. All rights reserved.
doi:10.1016/j.jhydrol.2008.10.014

**Nomenclature**

| | |
|---|---|
| $K$ | hydraulic conductivity of aquifer, [$LT^{-1}$] |
| $K'$ | hydraulic conductivity of zone of influence, [$LT^{-1}$] |
| $S_s$ | specific storage of aquifer, [$L^{-1}$] |
| $S_s'$ | specific storage of zone of influence, [$L^{-1}$] |
| $\alpha$ | hydraulic diffusivity of aquifer, [$L^2T^{-1}$] |
| $\alpha'$ | hydraulic diffusivity of zone of influence, [$L^2T^{-1}$] |
| $\alpha_w$ | hydraulic diffusivity of well, [$L^2T^{-1}$] |
| $b$ | aquifer thickness, [L] |
| $r$ | radial distance from center of observation well, [L] |
| $r^*$ | radial distance from pumping well, [L] |
| $r_w$ | radius of observation well, [L] |
| $r_\infty$ | radius of observation well zone of influence, [L] |
| $r^*_{obs}$ | radial distance of observation well from pumping well, [L] |
| $\hat{s}$ | drawdown in zone of influence, [L] |
| $s$ | drawdown outside zone of influence, [L] |
| $Q$ | pumping well discharge rate, [$L^3T^{-1}$] |
| $p$ | Laplace transform parameter |
| $t$ | time since onset of pumping, [T] |
| $\theta$ | local observation well tangential coordinate, [radians] |

wellbore skin in which hydraulic head varies linearly with radial distance, as shown by the dashed–dotted lines in Fig. 1a. In this case, one expresses the basic time lag, $t_B$, as a function of the hydraulic conductivity of wellbore skin, $K_s$, instead of the formation hydraulic conductivity, $K$. The parameter $F$ is said to represent the flow field geometry around the observation well (see Holden and Burt (2003) and references therein) and may then be viewed as a characteristic length dimension of wellbore skin. For cases with no wellbore skin $F$ is simply a fitting parameter with no clear physical meaning.

A shortcoming of the model of Black and Kipp (1977) is that the measuring instrument only affects the formation flow field at the wellbore or within the radial extent of wellbore skin. This means that, outside the wellbore, in the absence of wellbore skin, the formation response is that predicted by the Theis (1935) solution. In the presence of wellbore skin, Black and Kipp (1977) assume head distribution in the skin is linear, which is a consequence of neglecting the specific storage of wellbore skin. The assumption of negligible skin storage is sufficient only when the radial extent of skin is relatively small. However, even when this assumption is valid, the zone of the formation flow field influenced by the presence of an observation well may not be limited to wellbore skin, particularly for cases where wellbore skin is highly conductive.

In this work, we propose a solution that allows for head continuity at the wellbore–formation interface and is thus less approximate than the theory of Hvorslev (1951) used in Black and Kipp (1977). A schematic of the conceptual model used to develop the solution is shown in Fig. 1b. Head continuity is maintained at the wellbore–formation interface without the introduction of fitting parameters such as the the shape factor of Hvorslev (1951) and Black and Kipp (1977). As a consequence of enforcing continuity of head at the wellbore–formation interface, the solution developed here predicts drawdown that varies with position (i.e. in the tangential direction) around the wellbore. The variation is very slight and when averaged around the wellbore circumference, yields the hydraulic head that is a predictor of what is measured by a transducer placed in the wellbore.

The solution developed here was fitted to field data from Black and Kipp (1977) using the drawdown and drawdown time derivative based type-curve approaches. The drawdown based type-curve approach follows that of Black and Kipp (1977), where as the derivative based approach follows the works of Illman and Neuman (2000, 2001). The derivative based method is known to accentuate wellbore storage effects allowing for more unique estimates in cases where drawdown based type-curves are not significantly dissimilar for different parameter values. The drawdown based approach was found to yield an estimate of aquifer hydraulic diffusivity that is comparable but not equal to that obtained by Black and Kipp (1977). Despite the similarity in estimated parameter values, it should be noted that the solution developed in this work can, in addition to yielding estimates of formation conductivity and specific storage, yields estimates of the hydraulic conductivity and specific storage of the zone of influence. The solution also has the ability to predict the effect of the observation well on drawdown response in a finite region of influence in the vicinity of the well. Parameters were also estimated using the derivative based type-curve approach. The hydraulic diffusivity of the aquifer estimated according to this approach is of the same order of magnitude as that estimated with the drawdown based method.

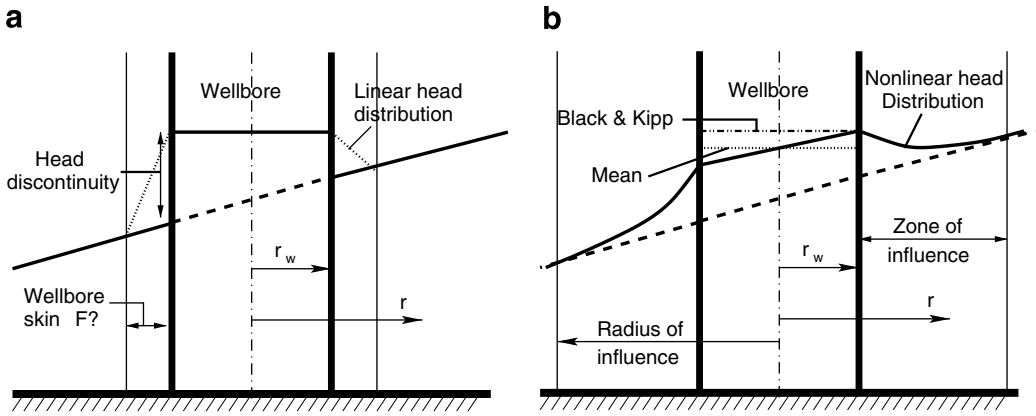


**Figure 1.** Schematics of the conceptual models for wellbore flow dynamics. (a) Black and Kipp (1977), and (b) proposed model. Solid curves are model predicted response and dashed curves are the Theis solution. Dotted line in (b) is mean wellbore drawdown of proposed model.

## Proposed approach

We consider flow in the zone of influence of an observation well that is emplaced in a homogeneous confined aquifer of thichkness $b$ and infinite radial extent that is pumped at a constant rate. The governing equation for flow in the zone of observation well influence is given by

$$\frac{1}{\alpha'}\frac{\partial \hat{s}}{\partial t}=\frac{1}{r}\frac{\partial}{\partial r}\left(r\frac{\partial \hat{s}}{\partial r}\right)+\frac{1}{r^2}\frac{\partial^2 \hat{s}}{\partial \theta^2}, \tag{1}$$

where $\hat{s}$ is drawdown in the zone of influence, $r$ is the radial distance from the center of the observation well, $\theta$ is the coordinate of the tangential flow direction, $t$ is time since the start of pumping, $\alpha'=K'/S_s'$, with $K'$ and $S_s'$ being, respectively, the hydraulic conductivity and specific storage of the zone of influence of the observation well. Outside the zone of influence, we use the notation $s$ for drawdown, $K$ for hydraulic conductivity and $S_s$ for specific storage. The radial distance from the pumping well is denoted $r^*$. Drawdown outside the observation well zone of influence is assumed to satisfy the solution of Theis (1935). Eq. (1), for drawdown in the observation well zone of influence, is solved subject to the initial condition

$$\hat{s}(r,\theta,0)=0, \tag{2}$$

based on the assumption that the system is initially static, and the boundary conditions

$$\hat{s}(r_\infty,\theta,t)=s(\theta,t), \tag{3}$$

at the edge of the zone of influence, and

$$2\pi bK'\left(r\frac{\partial \hat{s}}{\partial r}\right)\Big|_{r=r_w}=C_w\frac{\partial \hat{s}}{\partial t}\Big|_{r=r_w}, \tag{4}$$

at the wellbore, where $C_w$ is the wellbore storage coefficient, which, for open wells, is taken to be $C_w=\pi r_w^2$, where $r_w$ is the radius of the well (or well casing). The nonhomogeneous Dirichlet boundary condition given in Eq. (3) uses the Theis solution as the forcing function at the edge of the zone of influence. The boundary condition at the wellbore accounts for the effect of finite wellbore radius and wellbore storage.

In the tangential flow direction, we impose the following periodicity conditions:

$$\hat{s}(r,\pi,t)=\hat{s}(r,-\pi,t), \tag{5}$$

and

$$\frac{\partial \hat{s}}{\partial \theta}\Big|_{\theta=\pi}=\frac{\partial \hat{s}}{\partial \theta}\Big|_{\theta=-\pi}. \tag{6}$$

These periodicity conditions at $\theta=\pm\pi$ ensure continuity of hydraulic head and fluid flux at $\theta=\pm\pi$ since points on the line $\theta=\pi$ are the same as those on the line $\theta=-\pi$.

In dimensionless form, we write the above flow problem as

$$\frac{1}{\alpha_D}\frac{\partial \hat{s}_D}{\partial t_D}=\frac{1}{r_D}\frac{\partial}{\partial r_D}\left(r_D\frac{\partial \hat{s}_D}{\partial r_D}\right)+\frac{1}{r_D^2}\frac{\partial^2 \hat{s}_D}{\partial \theta^2}, \tag{7}$$

$$\hat{s}_D(r_D,\theta,0)=0, \tag{8}$$

$$\hat{s}_D(r_{D,\infty},\theta,t_D)=s_D(\theta,t_D), \tag{9}$$

$$\left(r_D\frac{\partial \hat{s}_D}{\partial r_D}\right)\Big|_{r_D=r_{D,w}}=\frac{1}{\alpha_{D,w}}\frac{\partial \hat{s}_D}{\partial t_D}\Big|_{r_D=r_{D,w}}, \tag{10}$$

$$\hat{s}_D(r_D,\pi,t_D)=\hat{s}_D(r_D,-\pi,t_D), \tag{11}$$

and

$$\frac{\partial \hat{s}_D}{\partial \theta}\Big|_{\theta=\pi}=\frac{\partial \hat{s}_D}{\partial \theta}\Big|_{\theta=-\pi}, \tag{12}$$

**Table 1**
Dimensionless variables and parameters.

| |
|---|
| $\hat{s}_D=\hat{s}/[Q/(4\pi bK)]$ |
| $r_D=r/b$ |
| $r_D^*=r^*/b$ |
| $r_{D,\mathrm{obs}}^*=r_{\mathrm{obs}}^*/b$ |
| $r_{D,\infty}^*=r_\infty^*/b$ |
| $r_D'=r/r_w$ |
| $r_{D,\infty}'=r_\infty'/r_w$ |
| $t_D=\alpha t/b^2$ |
| $\alpha_D=\alpha'/\alpha$ |
| $\alpha_{D,w}=\alpha_w/\alpha$ |

where $\hat{s}_D=\hat{s}/[Q/(4\pi bK)]$, $r_D=r/b$, $r_{D,w}=r_w/b$, $t_D=\alpha t/b^2$, $\alpha=K/S_s$ is the hydraulic diffusivity of the aquifer, $\alpha_D=\alpha'/\alpha$ is the dimensionless hydraulic diffusivity of the zone of influence, $\alpha_{D,w}=\alpha_w/\alpha$ and $\alpha_w=2\pi b^3K'/C_w$. A summary of the dimensionless variables and parameters used in this work is given in Table 1.

## Solution

The Laplace transform of drawdown in the observation well and in its immediate vicinity (region of influence) is given by the following complete Fourier series (see Appendix for details of derivation):

$$\bar{\hat{s}}_D(z,\theta)=\bar{a}_0(z)+\sum_{n=1}^{\infty}\left[\bar{a}_n(z)\cos(n\theta)+\bar{b}_n(z)\sin(n\theta)\right], \tag{13}$$

where $z=r_D\sqrt{p/\alpha_D}$ and the Fourier series coefficients are given by

$$\bar{a}_0(z)=\frac{\bar{u}_0(z)}{2\pi}\int_{-\pi}^{\pi}\bar{s}_D(\theta,p)\mathrm{d}\theta, \tag{14}$$

$$\bar{a}_n(z)=\frac{\bar{u}_n(z)}{\pi}\int_{-\pi}^{\pi}\bar{s}_D(\theta,p)\cos(n\theta)\mathrm{d}\theta \tag{15}$$

$$\bar{b}_n(z)=\frac{\bar{u}_n(z)}{\pi}\int_{-\pi}^{\pi}\bar{s}_D(\theta,p)\sin(n\theta)\mathrm{d}\theta \tag{16}$$

for $n=1,2,3,\ldots$, and

$$\bar{u}_n(z)=\frac{I_n(z)-\omega_nK_n(z)}{I_n(z_\infty)-\omega_nK_n(z_\infty)} \tag{17}$$

for $n=0,1,2,\ldots$,

$$\omega_n=\frac{(n-p/\alpha_{D,w})I_n(z_w)+z_wI_{n+1}(z_w)}{(n-p/\alpha_{D,w})K_n(z_w)-z_wK_{n+1}(z_w)}, \tag{18}$$

with $z_w=r_{D,w}\sqrt{p/\alpha_D}$ and $z_\infty=r_{D,\infty}\sqrt{p/\alpha_D}$.

In principle, inverting the Laplace transform of $\bar{\hat{s}}(r,\theta,p)$ given in Eq. (13) analytically leads to

$$\hat{s}_D(r_D,\theta,t_D)=a_0(r_D,t_D)+\sum_{n=1}^{\infty}[a_n(r_D,t_D)\cos(n\theta)+b_n(r_D,t_D)\times\sin(n\theta)], \tag{19}$$

where

$$a_0(r_D,t_D)=\frac{1}{2\pi}\int_0^{t_D}u_0(r_D,\tau_D)\int_{-\pi}^{\pi}s_D(\theta,t_D-\tau_D)\mathrm{d}\theta\mathrm{d}\tau_D, \tag{20}$$

and

$$a_n(r_D,t_D)=\frac{1}{\pi}\int_0^{t_D}u_n(r_D,\tau_D)\int_{-\pi}^{\pi}s_D(\theta,t_D-\tau_D)\cos(n\theta)\mathrm{d}\theta\mathrm{d}\tau_D \tag{21}$$

$$b_n(r_D,t_D)=\frac{1}{\pi}\int_0^{t_D}u_n(r_D,\tau_D)\int_{-\pi}^{\pi}s_D(\theta,t_D-\tau_D)\sin(n\theta)\mathrm{d}\theta\mathrm{d}\tau_D \tag{22}$$

for $n=1,2,3,\ldots$, where $u_n(r_D,t_D)=\mathscr{L}^{-1}\{\bar{u}_n(r_D,p)\}$. For our purposes, $s_D(\theta,t_D)$ is the Theis solution given by

$$s_D(\theta, t_D) = E_1\left(\frac{r_D^{*2}(\theta)}{4t_D}\right). \quad (23)$$

where

$$r_D^{*2}(\theta) = r_{D,\mathrm{obs}}^{*2} + r_{D,\infty}^2 + 2r_{D,\mathrm{obs}}^* r_{D,\infty} \cos(\theta). \quad (24)$$

An alternative to analytical inversion of the Laplace transform of $\bar{s}(r, \theta, p)$ is numerical. Numerical algorithms for inverting Laplace transforms include the methods of Stehfest (1970), Crump (1976), Talbot (1979) and de Hoog et al. (1982). In this work the method of Talbot (1979) is used due to the relative simplicity of its implementation.

## Model predicted system behavior

We have introduced here the parameter $r_\infty$ to denote the radius of influence of an observation well. Fig. 2 shows that as one moves toward the edge of the region of influence, that is, as $r_D$ approaches $r_{D,\infty}$, the solution developed here approaches the Theis (1935) solution. As expected, the most departure from the Theis solution is at the observation well ($r_D = 5 \times 10^{-3}$ in the figure). One can develop an empirical equation for $r_\infty$ of the form $r'_{D,\infty} = f(\alpha_D, \alpha_{D,w})$ where $r'_{D,\infty} = r_\infty / r_w$. In Fig. 3 we plot the predicted response in the well for different values of $r'_{D,\infty}$. The plots in Fig. 3a and (b) show that the solution converges at different values of $r'_{D,\infty}$ for different values of $\alpha_{D,w}$. The results indicate that $r'_{D,\infty}$ decreases with increasing $\alpha_{D,w}$. For instance, for the case of $\alpha_D = 10^{-1}$ (Fig. 3a), the curves are more spread out and the solution converges at $r'_{D,\infty} > 60$, indicating that an observation well of radius 5 cm would have a radius of influence of greater than 3 m, whereas for the case of $\alpha_D = 10^1$ (Fig. 3a), convergence is achieved at $r'_{D,\infty} \leqslant 60$. These results also show that when analyzing pumping test data from closely spaced observation wells, interaction between the wells should be taken into account. The solution developed here accounts for impact of an observation well on flow in the formation.

In Fig. 4 we plot the response of observation wells at different dimensionless radial distances, $r^*_{D,\mathrm{obs}}$ from the pumping well. The figure shows that instrument delay, relative to the response predicted by the Theis (1935) solution, decreases with increasing distance of the observation well from the pumping well, a fact also noted by Narasimhan and Zhu (1993). Thus, for a confined aquifer of thickness $b = 10$ m, the response of an observation well located 60 m from the pumping well would be virtually indistinguishable from that predicted by the Theis (1935) solution. The figure is included here to demonstrate that the solution developed in this work is consistent with known confined aquifer flow theory, tending to the Theis solution as the observation well distance from the pumping well increases.

Fig. 5 shows the predicted response in the neighborhood of the observation well. Dimensionless drawdown is plotted against the dimensionless radial distance, $r'_D = r/r_w$, from the observation well for different values of $\theta$. The figure shows the temporal evolution of drawdown response in the neighborhood of the well. The model results presented in the figure show that at early-time water flows

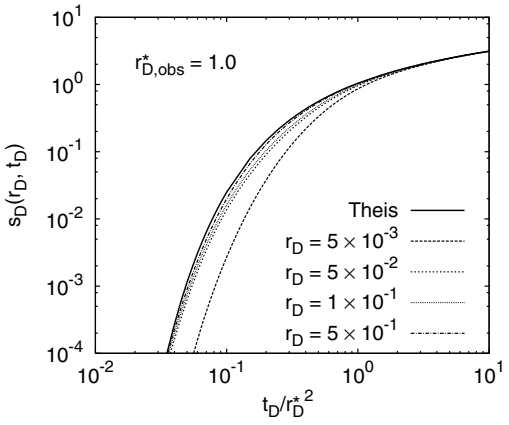


**Figure 2.** Log–log plot of dimensionless drawdown against $t_D/r_D^{*2}$ for different values of the dimensionless radial distance, $r_D < r_{D,\infty}$, from the observation well.

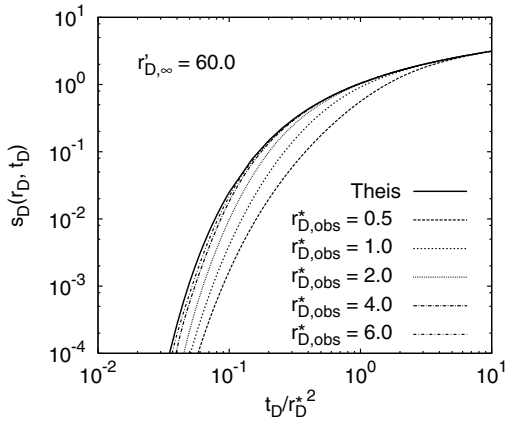


**Figure 4.** Log–log plot of dimensionless drawdown against $t_D/r_D^{*2}$ for different values of the dimensionless radial distance, $r^*_{D,\mathrm{obs}}$, from the pumping well.

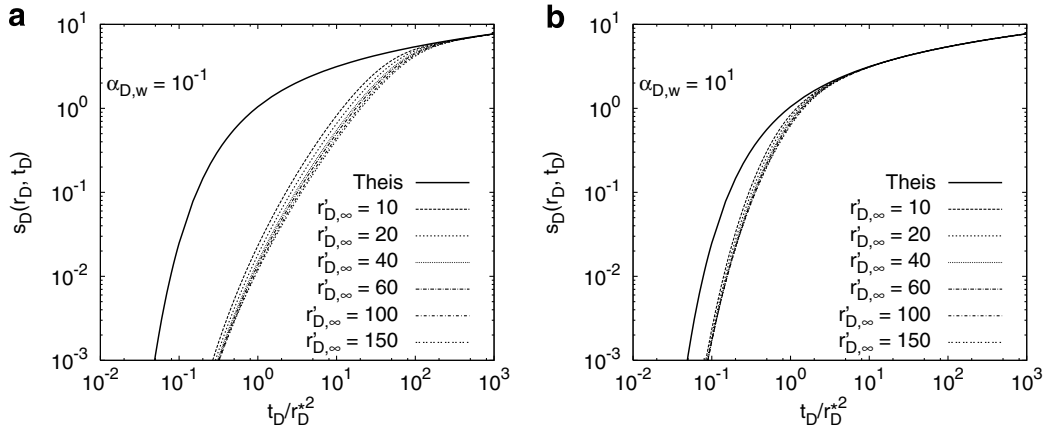


**Figure 3.** Log–log plot of dimensionless drawdown against $t_D/r_D^{*2}$ for different values of $r'_{D,\infty} = r_\infty/r_w$ for $\alpha_D = 1.0$, (a) $\alpha_{D,w} = 10^{-1}$ and (b) $\alpha_{D,w} = 10^1$.

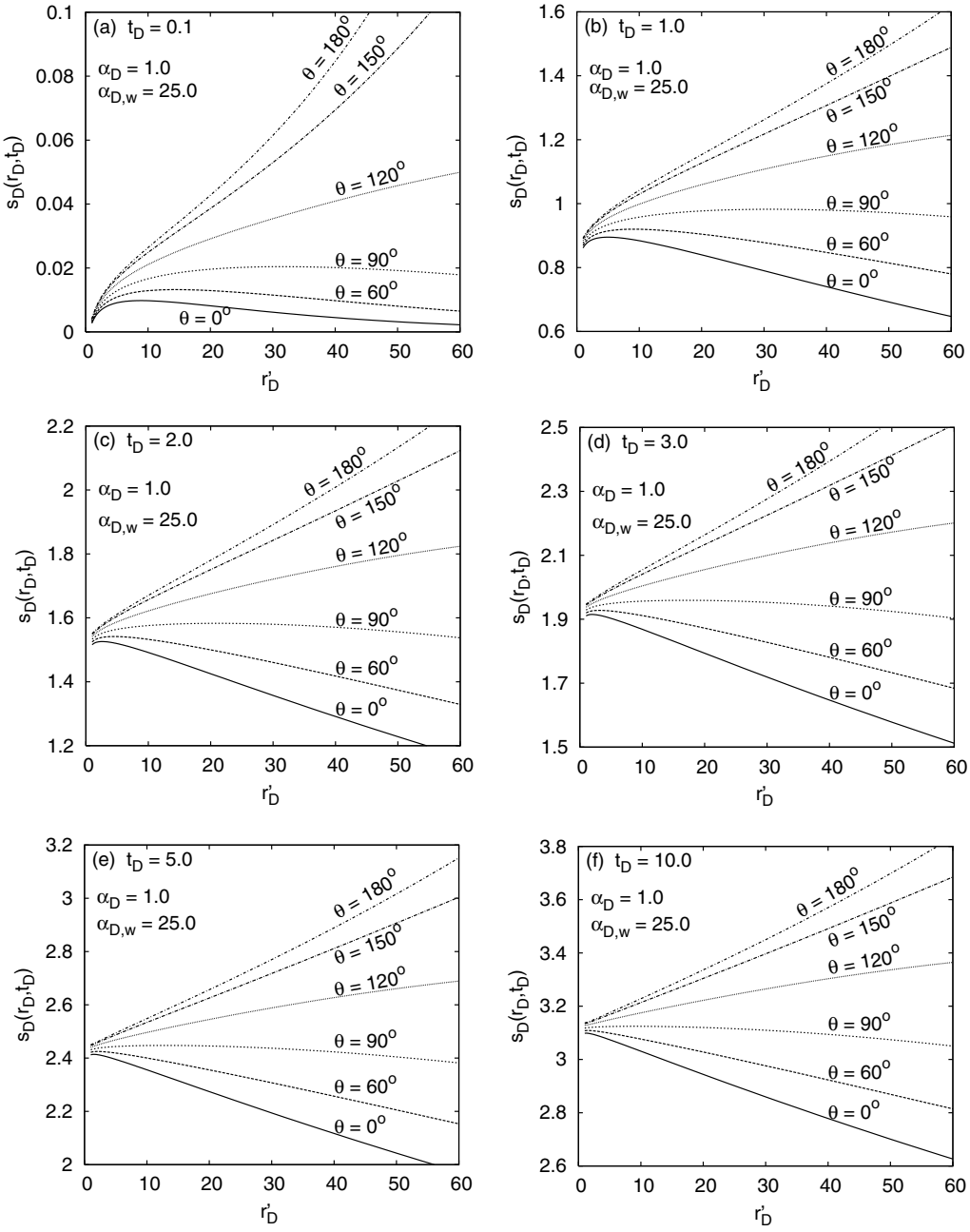


**Figure 5.** Plot of dimensionless drawdown against $r'_D$, the dimensionless radial distance from the observation well, for different values of $\theta$ at the indicated values of dimensionless time.

outward in all directions around the wellbore due to the delay in response of the observation well. At late time water flow in the observation well is unidirectional, always directed toward the pumping well as the observation well and the formation respond as a uniform medium. Considering a high conductivity ($K = 10^{-4}$ m/s) and low specific storage ($S_s = 10^{-6}$ m$^{-1}$) aquifer with a hydraulic diffusivity of $\alpha = 10^2$ m$^2$/s, as is typical of alluvial sand deposits, and having an initial saturated thickness of $b = 10$ m, Fig. 5 indicates that the unidirectional flow regime would be attainable after about 10 s. On the other hand, a moderately low conductivity ($K = 10^{-5}$ m/s) and high specific storage ($S_s = 10^{-4}$ m$^{-1}$) aquifer with a hydraulic diffusivity of $\alpha = 10^{-1}$ m$^2$/s, the unidirectional flow regime would be established after about 3 h.

Fig. 5 also shows that for $\theta \leqslant \pi/2$, drawdown decreases with increasing radial distance from the observation well. This is to be expected since for these angles, increasing radial distance from the observation well also corresponds to increasing distance from the pumping well, whereas the opposite is the case for $\theta > \pi/2$. The strong nonlinearity of drawdown in the neighborhood of the observation as predicted by our model and clearly observable in the model results at early-time, illustrates a siginificant difference between our solution and that of Black and Kipp (1977). It should be noted that the model of Black and Kipp (1977) predicts linear drawdown in the skin at all times, since the specific storage of the skin in ignored.

Black and Kipp (1977) introduced the dimensionless parameter $\beta$ which they referred to as the observation well response factor, defined as

$$\beta = \frac{4}{F_D}\left(\frac{C_w}{bS_s r^{*2}_{obs}}\frac{K}{K_s}\right) \tag{25}$$

where $F_D = F/b$ and $r^*_{obs}$ is the radial distance of the observation well from the pumping well. Similarly,

$$\frac{1}{r^{*2}_{D,obs}\alpha_{D,w}} = \frac{1}{2\pi}\left(\frac{C_w}{bS_s r^{*2}_{obs}}\frac{K}{K'}\right) \tag{26}$$

where $r^*_{D,obs} = r^*_{obs}/b$. In Fig. 6 we fit the solution of Black and Kipp (1977) to the response predicted by the solution developed in this work for $r_{D,obs} = 1.0$. For the results computed using our model with parameter values $\alpha_{D,w} = 1.75$ and 0.175, the fitted model of Black and Kipp (1977) yielded parameter values of $\beta$ = 10 and 100, respectively. These results suggest that, for parameter choices such that $\beta = 10/\alpha_{D,w}$, the two models produce virtually identical results, except at very early-time. Despite this similarity in predicted response in the well for $\beta = 10/\alpha_{D,w}$, it should be noted that the two models differ significantly in how they model the flow dynamics around the wellbore. The most significant advancement introduced by our solution is the ability to predict drawdown response in the immediate vicinity of the observation well, which is critical in analyzing flow and transport of contaminants in a wellfield with closely spaced observation wells.

Fig. 7 shows the effect of $\alpha_D$ on the response of the obserevation well for $\alpha_{D,w} = 24.0$, which corresponds to a 5 cm-diameter observation well. The results in the figure indicate that the delay in response of the observation well decreases with increasing values of $\alpha_D$, the ratio of the hydraulic diffusivity of the zone of influence to that of the aquifer. This implies that as the hydraulic conductivity of the zone of influence increases or as the specific storage decreases relative to that of the formation outside the zone of influence, the delay in response of the observation well decreases, as one would expect.

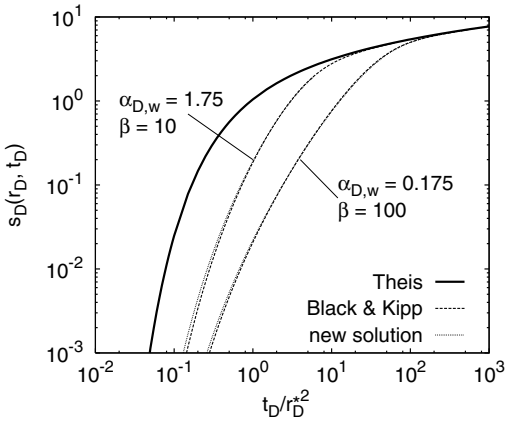


**Figure 6.** A comparison of predicted response of the new model (for $\alpha_{D,w} = 1.75, 0.175$) to the solution of Black and Kipp (1977) (for $\beta = 10, 100$).

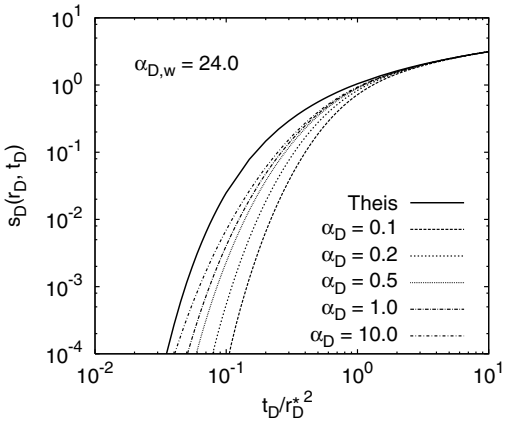


**Figure 7.** Log–log plot of dimensionless drawdown against $t_D/r^2_D$ for different values of the dimensionless hydraulic diffusivity, $\alpha_D$, of the observation well region of influence.

## Application to field data

For the solution developed here, the dimensionless parameter $1/(r^{*2}_{D,obs}\alpha_{D,w})$ can be used as a measure of the observation well response time. Fig. 8a shows the model predicted response for different values of the parameter $\alpha_{D,w}$ for the case of $\alpha_D = 1.0$ and $r_{D,obs} = 1.0$. This plot can be used in type-curve estimation of aquifer parameters in a manner akin to the approach of Black and Kipp (1977). When the type-curves are not sufficiently dissimilar for different values of the dimensionless parameter $\alpha_{D,w}$ it may to non-unique estimates of hydraulic parameters. In such a case it may be appropriate to adopt the approach of Illman and Neuman (2000, 2001) who proposed the use of type-curves of the derivative of dimensionless drawdown with respect to the natural log of $t_D$, i.e.

$$\frac{\partial \hat{s}_D}{\partial \ln t_D} = t_D \frac{\partial \hat{s}_D}{\partial t_D}. \tag{27}$$

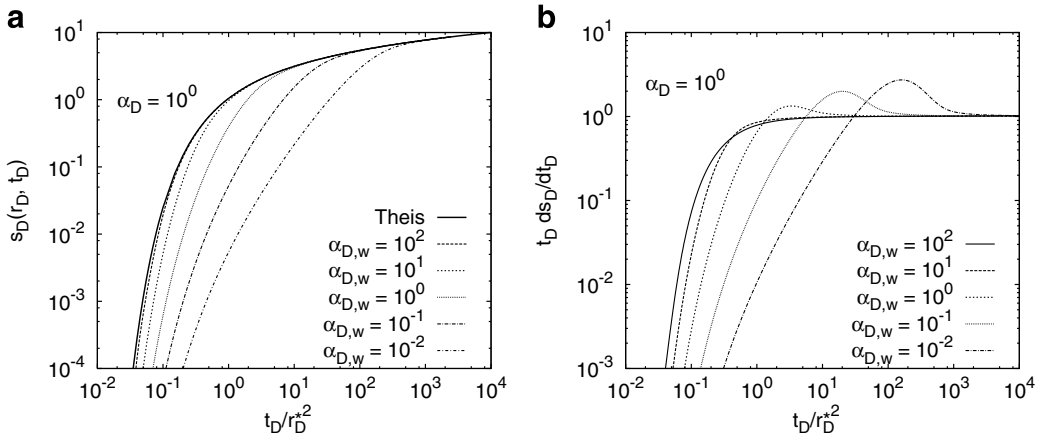


**Figure 8.** Log–log plot of (a) dimensionless drawdown against $t_D/r^2_D$ and (b) the derivative of dimensionless drawdown with respect to $\ln(t_D)$, for different values of the dimensionless parameter $\alpha_{D,w}$.

Fig. 8b shows log–log plots of the derivative of $\hat{s}_D$ with respect to the natural log of $t_D$ for different values of $\alpha_{D,w}$. As can be seen in the figure, and in harmony with the work of Illman and Neuman (2000, 2001), the derivative approach accentuates the differences between type-curves of different values of $\alpha_{D,w}$.

Using pumping test data from Black and Kipp (1977) and the solution developed here, we estimate the model parameters and compare them to those obtained by Black and Kipp (1977). We use the type-curve approach in the manner of Black and Kipp (1977) to estimate the parameters. The main difference with the type-curve approach of Black and Kipp (1977) is that, for the model developed here, one has to generate multiple type-curve plots, of the form shown in Fig. 8, for different values of $\alpha_D$, the hydraulic diffusivity of the zone of influence. The drawdown based type-curve approach is used here for illustrative purposes. Fig. 9 shows the results of drawdown based type-curve procedure. The data fit shown in the figure was obtained for the dimensionless parameter values of $\alpha_D = 0.1$ and $\alpha_{D,w} = 1.0$. The coordinates of the match point are $(\hat{s}_D, t_D/r_D^{*2}) = (10, 1)$ and $(\hat{s}, t) = (28.0, 0.445)$. Given that $r^*_{\text{obs}} = 80$ m, the hydraulic diffusivity of the aquifer is $\alpha = 2.28 \times 10^3$ m$^2$/min. Black and Kipp (1977) obtained $\alpha = 2.44 \times 10^3$ m$^2$/min, which compares well to the estimate obtained here. Additionally, given the aquifer thickness $b = 83$ m, the hydraulic conductivity of the aquifer is $K = 2.24Q \times 10^{-3}$ m/min, where $Q$ is pumping well discharge rate. Hence, given the pumping rate, estimates for aquifer hydraulic conductivity and specific storage can be obtained. The ratio $\alpha_D/\alpha_{D,w} = 0.1$ leads to $S'_s = 5C_w/(\pi b^3)$ for the specific storage of the region of influence. Hence, given the wellbore storage coefficient $C_w$, one can estimate the parameters $K'$ and $S'_s$.

The derivative of drawdown data with respect to $\ln(t)$ was approximated using central differences, and the results of the derivative based type-curve fit are shown in Fig. 10. The best fit was obtained for dimensionless parameter values of $\alpha_D = 10^{-2}$ and $\alpha_{D,w} = 10^{-1}$, both of which are an order of magnitude smaller than the respective values obtained with the drawdown based type-curve method. Using coordinates of the match point shown in the figure, estimates of $\alpha = 7.57 \times 10^3$ m$^2$/min and $K = 5.58Q \times 10^{-3}$ m/min for the aquifer hydraulic diffusivity and conductivity, respectively. As in the above analysis, $S'_s = 5C_w/(\pi b^3)$. The differences in parameter estimates yielded by the two type-curve methods illustrate the fact that the derivative approach tends to accentuate the differences between type-curves corresponding to different values of the parameter $\alpha_{D,w}$. Despite the greater noise level in the derivative data, it is still easier to graphically distinguish between type-curves than with traditional type-curve approach. The type-curve methods illustrated here both yield estimates of parameters $K$, $K'$, $S_s$ and $S'_s$, given the pumping rate and the wellbore storage coefficient.

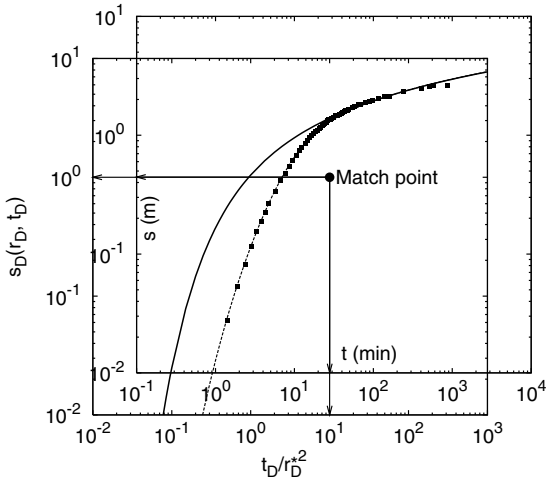


**Figure 9.** Type-curve fit of observed drawdown data (after Black and Kipp (1977)), with match point coordinates of $(t_D/r_D^{*2}, \hat{s}_D) = (10, 1)$ and $(t, s) = (28.0, 0.445)$.

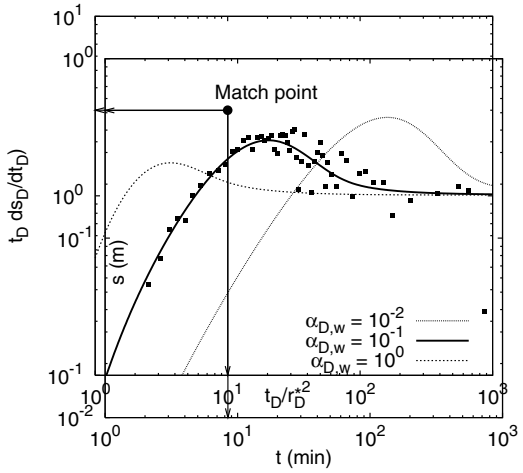


**Figure 10.** Derivative based type-curve fit to the derivative of drawdown data (after Black and Kipp (1977)) with respect to $\ln(t_D)$. The match point coordinates are $(t_D/r_D^{*2}, t_D\partial\hat{s}_D/\partial t_D) = (10, 3)$ and $(t, t\partial s/\partial t) = (8.45, 0.52)$.

## Conclusion

We have proposed here a solution that allows for head continuity at the wellbore–formation interface leading to drawdown at the wellbore–formation interface that varies with position (i.e. in the tangential direction) around the wellbore. This variation of head with position around the wellbore, slight as it may be, yields the hydraulic gradients necessary to generate the flow of fluid through the wellbore. Mathematically, this variation arises due to the forcing function at $r_\infty$, the Theis solution, which is a function of $\theta$ in the local observation well coordinate system. The solution developed in this work can, in addition to estimates of formation conductivity and specific storage, yield estimates of the hydraulic conductivity and specific storage of the zone of influence. The solution also has the ability to predict the effect of the observation well on drawdown response in a finite region of influence in the vicinity of the well. This is what sets it apart from the model of Black and Kipp (1977), which modifies formation response only at the observation well. The ability to model nonlinear fluid flow in the vicinity of a observation well is critical when analyzing flow and transport of contaminants in a wellfield with closely spaced wells.

The type-curve approach of the form used by Black and Kipp (1977) can also be used with the model developed here using the type-curves shown in Fig. 8. The type-curves are a family of curves corresponding to different values of $\alpha_{D,w}$. For cases where these type-curves are not significantly different for different values $\alpha_{D,w}$ the ambiguity in the graphical estimation of hydraulic parameters may be minimized by used of derivative based type-curves proposed by Illman and Neuman (2000, 2001). The type-curves based on the derivative of drawdown with respect to the natural log of time are known to accentuate wellbore storage effects allowing for more unique parameter estimates in cases where drawdown based type-curves are not significantly dissimilar for different parameter values. However, a measure of ambiguity still remains in selecting the value $\alpha_D$ given that field data may fit type-curves of different values of $\alpha_D$ equally well. In such instances it may be more preferable to use parameter estimation routines such as PEST Doherty (2002).

## Appendix A

Using the method of separation of variables, since Eq. (7) is linear and homogeneous and the boundary conditions in $\theta$ are homogeneous, we decompose $\hat{s}_D$ as

$$\hat{s}_D(r_D,\theta,t_D) = \hat{s}_{D,1}(\theta)\hat{s}_{D,2}(r_D,t_D), \tag{A.1}$$

and substitute this into Eq. (1). This leads to the following eigenvalue problem:

$$\frac{d^2\hat{s}_{D,1}}{d\theta^2} + \lambda\hat{s}_{D,1} = 0, \tag{A.2}$$

where $\lambda$ is the separation constant. Eq. (A.2), to determine the separation constant, is solved subject to periodicity conditions

$$\hat{s}_{D,1}(\theta=\pi) = \hat{s}_{D,1}(\theta=-\pi), \tag{A.3}$$

and

$$\left.\frac{d\hat{s}_{D,1}}{d\theta}\right|_{\theta=\pi} = \left.\frac{d\hat{s}_{D,1}}{d\theta}\right|_{\theta=-\pi}. \tag{A.4}$$

Separation of variables also leads to the following equation for $\hat{s}_{D,2}(r_D,t_D)$:

$$\frac{1}{\alpha_D}\frac{\partial\hat{s}_{D,2}}{\partial t_D} = \frac{1}{r_D}\frac{\partial}{\partial r_D}\left(r_D\frac{\partial\hat{s}_{D,2}}{\partial r_D}\right) - \frac{\lambda}{r_D^2}\hat{s}_{D,2}, \tag{A.5}$$

which is solved subject to

$$\hat{s}_{D,2}(r_D,0) = 0, \tag{A.6}$$

$$\hat{s}_{D,2}(r_{D,\infty},\lambda,t_D) = s_D(\lambda,t_D), \tag{A.7}$$

$$\left(r_D\frac{\partial\hat{s}_{D,2}}{\partial r_D}\right)\Big|_{r_D=r_{D,w}} = \frac{1}{\alpha_{D,w}}\left.\frac{\partial\hat{s}_{D,2}}{\partial t_D}\right|_{r_D=r_{D,w}}. \tag{A.8}$$

Solving the eigenvalue problem given in Eqs. (A.2)–(A.4) yields the eigenvalues $\lambda_n = n^2$, with $n = 0,1,2,\ldots$, and the eigenfunctions

$$\hat{s}_{D,1} \backsim \{\cos(n\theta),\sin(n\theta)\}. \tag{A.9}$$

Note that the case $n = 0$, which corresponds to a constant in $\theta$ being an eigenfunction, is also included. Further, taking the Laplace transform of Eqs. (A.5) and (A.8), applying the initial condition in Eq. (A.6) and setting $z = r_D\sqrt{p/\alpha_D}$, where $p$ is the Laplace transform parameter, leads to

$$z^2\frac{d^2\bar{\hat{s}}_{D,2}}{dz^2} + z\frac{d\bar{\hat{s}}_{D,2}}{dz} - (z^2+n^2)\bar{\hat{s}}_{D,2} = 0, \tag{A.10}$$

and

$$\left(z\frac{d\bar{\hat{s}}_{D,2}}{dz} - \frac{p}{\alpha_{D,w}}\bar{\hat{s}}_{D,2}\right)\Big|_{z=z_w} = 0, \tag{A.11}$$

where $z_w = r_{D,w}\sqrt{p/\alpha_D}$. The solution to Eq. (A.10) subject to (A.11) is

$$\bar{\hat{s}}_{D,2} = c[I_n(z) - \omega_n K_n(z)], \tag{A.12}$$

where $c$ is an arbitrary constant in $z$, $I_n(z)$ and $K_n(z)$ are the $n$th-order modified Bessel functions of the first and second kind, respectively.

## References


Black, J.H., Kipp Jr., K.L., 1977. Observation well response time and its effect upon aquifer tests. Journal of Hydrology 34, 297–306.

Boulton, N. S., 1954. The drawdown of the water-table under non-steady conditions near a pumped well in an uncofined formation. In: Proceeding, Institution of Civil Engineers. vol. 3, pp. 564–579.

Boulton, N.S., Streltsova, T.D., 1976. The drawdown near an abstraction well of large diameter under non-steady conditions in an unconfined aquifer. Journal of Hydrology 30, 29–46.

Crump, K.S., 1976. Numerical inversion of laplace transforms using a fourier series approximation. Journal of the Association for Computing Machinery 23 (1), 89–96.

de Hoog, F.R., Knight, J.H., Stokes, A.N., 1982. An improved method for numerical inversion of laplace transforms. SIAM Journal of Scientific and Statistical Computing 3 (3), 357–366.

Doherty, J., 2002. Manual for PEST, fifth ed. Watermark Numerical Computing, Australia.

Holden, J., Burt, T.P., 2003. Hydraulic conductivity in upland blanket peat: measurement and variability. Hydrological Processes 17, 1227–1237.

Hvorslev, M.J., 1951. Time lag and soil permeability in ground-water observations. US Army Corps of Engineers, Waterways Experiment Station, Vicksburg, Mississippi, Bulletin 36.

Illman, W.A., Neuman, S.P., 2000. Type-curve interpretation of multivariate single-hole pneumatic injection tests in unsaturated fractured rock. Ground Water 38 (6), 899–911.

Illman, W.A., Neuman, S.P., 2001. Type-curve interpretation of a cross-hole pneumatic injection test in unsaturated fractured tuff. Water Resources Research 37 (3), 583–603.

Moench, A.F., 1997. Flow to a well of finite diameter in a homogeneous, anisotropic water table aquifer. Water Resources Research 33 (6), 1397–1407.

Mucha, I., Paulikova, E., 1986. Pumping test using large-diameter production and observation wells. Journal of Hydrology 89, 157–164.

Narasimhan, T.N., Zhu, M., 1993. Transient flow of water to a well in an unconfined aquifer: applicability of some conceptual models. Water Resources Research 29 (1), 179–191.

Neuman, S.P., 1972. Theory of flow in unconfined aquifers considering delayed response of the water table. Water Resources Research 8 (4), 1031–1045.

Papadopulos, I.S., Cooper, H.H., 1967. Drawdown in a well of large diameter. Water Resources Research 3 (1), 241–244.

Stehfest, H., 1970. Numerical inversion of Laplace transforms. Communications of the ACM 13 (1), 47–49.

Talbot, A., 1979. The accurate numerical inversion of Laplace transforms. Journal of the Institute of Mathematics and its Applications 23, 97–120.

Theis, C.V., 1935. The relation between the lowering of the piezometric surface and the rate and duration of discharge of a well using ground-water storage. Transactions, American Geophysical Union 16, 519–524.